

# Short Papers

## Phase and Loss Characteristics of High Average Power Ferrite Phasers

J. L. ALLEN

**Abstract**—An analysis is presented of the propagation characteristics of some waveguide latching ferrite phaser structures useful for high average power applications. Calculated results show the effects on the loss and differential phase shift of adding vertical slab or T-shaped cooling structures of dielectrics, such as beryllium oxide and boron nitride. Typical design data are presented.

### INTRODUCTION

Analytical design data for low-power ferrite latching phase shifters have been reported by several authors [1]–[4]. The handling of high average RF power levels requires somewhat different designs. The principal difficulty is in dissipating the heat generated by losses in the ferrite. One design technique that has proven quite effective is the use of thermal conducting dielectrics [4], [5] placed against the vertical walls of the ferrite toroid and extended to the waveguide walls shown in Fig. 1. In Fig. 1(a), thermal conducting dielectric slabs are placed adjacent to the vertical ferrite walls and conduct heat to the broad waveguide walls. In Fig. 1(b), T-shaped thermal conducting dielectric elements are used to conduct heat from the ferrite to the narrow walls of the waveguide. The purpose of this short paper is to present typical results from an analysis of the structures of Fig. 1.

### ANALYSIS

The magnetic moments in the horizontal cross bars of the ferrite toroid are largely parallel to the RF magnetic field so that there is little interaction between the magnetization and the incident RF field. Thus for the purpose of analysis, the dielectric-loaded ferrite toroid may be modeled by a pair of oppositely magnetized ferrite slabs separated by a dielectric slab. When the dielectric core and the ferrite have the same dielectric constant, that value is used for the dielectric slab of the model. If the dielectric constant of the ferrite is different from that of the material in the toroid slot, an “effective” dielectric constant is computed for use in the model. Simple volumetric averages of the dielectric constant have been found to work quite well [3], [4]. In a similar fashion, the T-configuration of the dielectric can be modeled by a pair of slabs, one slab having an “effective” dielectric constant. The result is the vertical slab model for the high average power phaser shown in Fig. 2.

The characteristic equation for the vertical slab model can be determined by Seidel's [6] transfer-matrix method and is given by the following:

$$\left\{ \left[ (k_a k_b) (\cos k_a W_1) (\cos k_b W_2) + (-k_b^2) (\sin k_a W_1) (\sin k_b W_2) \right] \right. \\ \left. + \left[ \left( \frac{k_m}{\rho} \cos k_m W_3 - \frac{\gamma}{\rho \theta} \sin k_m W_3 \right) (\cos k_c W_4) \right. \right. \\ \left. + \left( \frac{-\sin k_m W_3}{\rho^2} \right) (k_c \sin k_c W_4) \right] \left. \right\} \\ + \left\{ \left[ (k_a \cos k_a W_1) (\sin k_b W_2) + (\sin k_a W_1) (k_b \cos k_b W_2) \right] \right. \\ \left. + \left\{ \left( \frac{-\gamma^2}{\theta^2} - k_m^2 \right) \sin k_m W_3 \right\} \{ \cos k_c W_4 \} \right. \\ \left. + \left\{ \frac{k_m}{\rho} \cos k_m W_3 + \frac{\gamma}{\rho \theta} \sin k_m W_3 \right\} \{ -k_c \sin k_c W_4 \} \right\} = 0 \quad (1)$$

where

$$\theta = j \frac{\langle \mu \rangle}{\langle \kappa \rangle} \quad \rho = \frac{\langle \mu \rangle}{\langle \mu \rangle^2 - \langle \kappa \rangle^2} \\ k_a^2 = \omega^2 \mu_0 \epsilon_0 \epsilon_a + \gamma^2 \quad k_b^2 = \omega^2 \mu_0 \epsilon_0 \epsilon_b + \gamma^2$$

Manuscript received February 9, 1972; revised March 15, 1973.  
The author is with the Electrical and Electronic Systems Department, University of South Florida, Tampa, Fla. 33620.

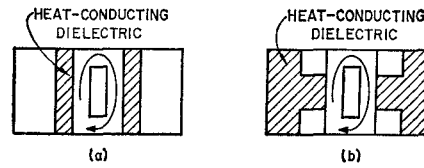


Fig. 1. Two configurations using heat conducting dielectrics to enhance high average power performance.

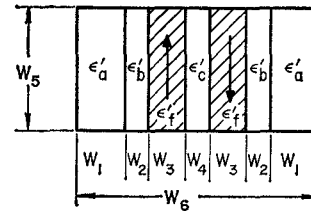


Fig. 2. Vertical slab model for the structures of Fig. 1.

	$\epsilon'_f = 16$ $\epsilon'_i = 16$ $\Delta H_i = 40 \text{ Oe}$ $f_c = 9 \text{ GHz}$ $R_r = 0.5$ $4\pi M_s = 1220 \text{ GAUSS}$
--	---

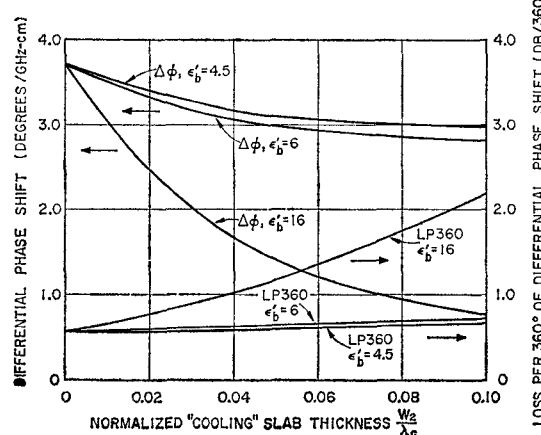


Fig. 3. Normalized loss and differential phase shift versus normalized cooling slab thickness.

$$k_c^2 = \omega^2 \mu_0 \epsilon_0 \epsilon_c + \gamma^2 \quad k_m^2 = \frac{\omega^2 \mu_0 \epsilon_0 \epsilon_f}{\rho} + \gamma^2. \\ \gamma = \alpha + j\beta$$

The ferrite in the latched state is described by  $\langle \mu \rangle$  and  $\langle \kappa \rangle$ , the components of the average permeability tensor [3]. Dielectric and magnetic losses are included directly in the boundary-value problem. Waveguide copper losses are not included in the computations. Numerical calculations were carried out on a CDC 6400 digital computer.

### NUMERICAL RESULTS

Equation (1) has been solved for a variety of material and structural parameters. Typical results are presented in normalized form in Figs. 3–5. The center frequency is designated  $f_c$ . All dimensions are in wavelengths.  $R_r$  is the remanence ratio and  $4\pi M_s$  is the saturation magnetization. The intrinsic linewidth is designated  $\Delta H_i$ . Fig. 3 illustrates the effect on differential phase shift and loss of adding cooling slabs of various thicknesses and dielectric constants. The values  $\epsilon'_b = 4.5$  and  $\epsilon'_b = 6$  correspond to boron nitride and beryllium oxide, respectively, both of which have good thermal properties. As

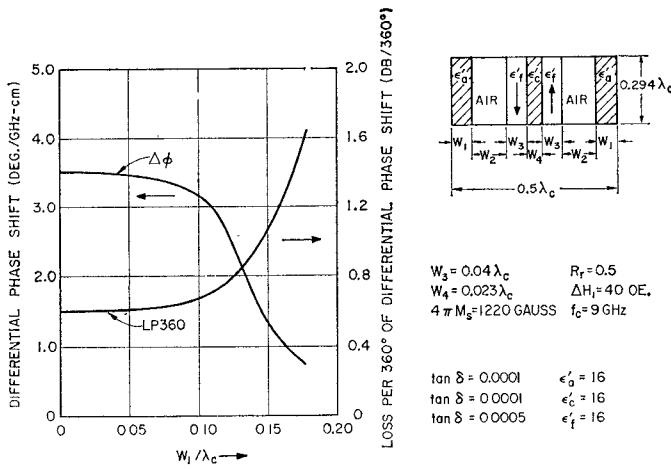


Fig. 4. Normalized loss and differential phase shift versus normalized slab width for slab against waveguide wall.

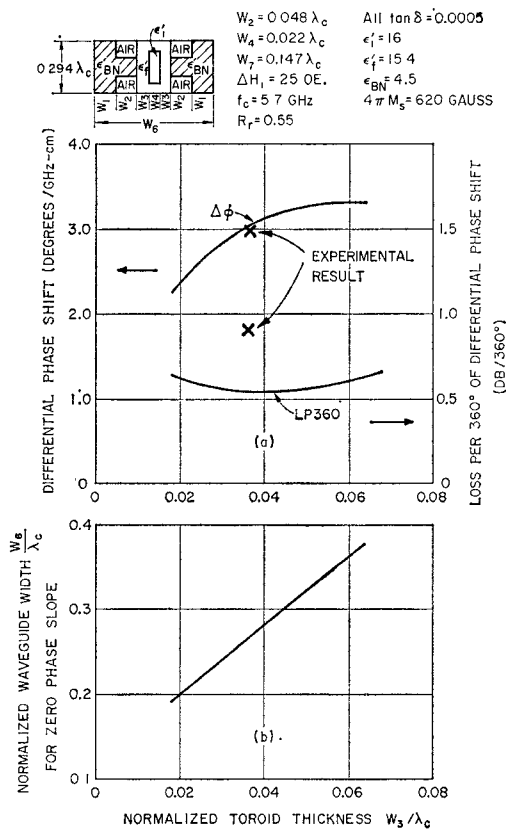


Fig. 5. (a) Normalized loss and differential phase shift versus normalized toroid wall thickness with constraint of zero phase slope. (b) Normalized waveguide width to produce zero phase slope for given value of toroid wall thickness.

can be seen from these curves, only a small sacrifice in phase shift and loss results from placing slabs of either of these materials against the toroid walls. The curve is included for reference and for  $\epsilon_a' = 16$  shows a rapid decrease in differential phase shift with increasing cooling slab thickness. The results given in Fig. 4 show that placing dielectric slabs against the waveguide walls has little effect on phase shift or loss until the slabs are quite thick (e.g., about  $0.1\lambda$  thick for  $\epsilon_a' = 16$ ).

Characteristics of a phaser with T-shaped cooling sections of boron nitride are shown in Fig. 5. In the calculations, the  $W_2$  region was replaced by an equivalent homogeneous slab with an effective dielectric constant calculated on a volume basis. Phasers are usually designed such that differential phase shift is independent of frequency

over the operating band, i.e., the phase slope is zero. The curves of Fig. 5(a) incorporate this constraint. Differential phase shift and loss are shown as a function of toroid wall thickness with the constraint that the waveguide width is adjusted for each value of toroid wall thickness to produce zero phase slope at the center frequency. The waveguide width required for zero phase slope is given in Fig. 5(b). Structures of this type are quite effective in increasing the average power handling capability of ferrite latching phasers [4]. Differential phase shift and insertion loss for an experimental C-band phaser are shown for comparison. Note that the calculated data do not include waveguide copper losses.

## CONCLUSION

An analysis has been presented of waveguide latching phaser structures useful for high average power applications. Calculated results show the effects on the loss and differential phase shift of adding vertical slab or T-shaped dielectric cooling structures. Design data presented permit a choice of toroid wall thickness and waveguide width to achieve optimum loss and phase characteristics with the constraint of zero phase slope.

## REFERENCES

- [1] E. Schliemann, "Theoretical analysis of twin-slab phase shifters in rectangular waveguide," *IEEE Trans. Microwave Theory Tech.*, vol. MTT-14, pp. 15-23, Jan. 1966.
- [2] W. J. Ince and E. Stern, "Computer analysis of ferrite digital phase shifters," in *IEEE Int. Conv. Rec.*, vol. 14, pt. 3, pp. 28-32, 1966.
- [3] J. L. Allen, "The analysis of ferrite phase shifters including the effects of losses," Ph.D. dissertation, Georgia Inst. Technol., Atlanta, May 1966.
- [4] G. P. Rodriguez, J. L. Allen, L. J. Lavedan, and D. R. Taft, "Operating dynamics and performance limitations of ferrite digital phase shifters," *IEEE Trans. Microwave Theory Tech.* (1967 Symposium Issue), vol. MTT-15, pp. 709-713, Dec. 1967.
- [5] Berger and Kapilevich, "Application of heat-removing ceramic dielectrics in SHF ferrite devices," *Radio Tekhnika*, vol. 25, pp. 79-83, 1971.
- [6] H. Seidel, "Ferrite slabs in transverse electric mode waveguide," *J. Appl. Phys.*, vol. 28, Feb. 1957.

## Low-Noise Microwave Down-Converter with Optimum Matching at Idle Frequencies

G. B. STRACCA, F. ASPESI, AND T. D'ARCANGELO

**Abstract**—A low-noise balanced down-converter for microwave radio-link applications is described. Down-converters of this type have been realized with typical noise figures of 3.5 dB at 4 GHz, 4 dB at 7 GHz, and 5 dB at 13 GHz. These results are obtained mainly by taking into account high order sideband frequencies of the pump harmonics up to the third, by properly terminating the image frequency, by matching the input port of the mixer and by optimizing the mixer-preamplifier interface. The experimental results are compared with the theoretical ones obtainable with ideal purely resistive diodes.

## I. INTRODUCTION

Theoretical analysis has shown that mixer performance depends not only on the RF/IF mixer impedances and on the image-frequency termination [1]-[4], but also on the terminations at the various "idle frequencies,"<sup>1</sup> as well as on the LO waveform [5]-[8].

This short paper describes a mixer configuration designed to control the idle-frequency terminations up to the third harmonic and gives experimental results for mixers operating at different frequency ranges (i.e., 3.6-4.2 GHz; 7.1-7.7 GHz; 12.7-13.3 GHz) which are now used in the receiving section of commercial radio links. Down-converters of the same type, operating at frequencies between 11 and 12 GHz, have also been developed for radiometric applications, and are presently in operation in various stations of the European Space Research Organization.

Manuscript received April 4, 1972; revised March 26, 1973.

G. B. Stracca is with the Istituto di Elettrotecnica ed Elettronica, Trieste University, Trieste, Italy.

F. Aspesi and T. D'Arcangelo are with the GTE Telecommunications Research Laboratories, Cassina de' Peppi, Milan, Italy.

<sup>1</sup> Idle frequencies are defined as follows:  $\omega_{+m} = m\omega_p \pm \omega_0$ , where  $\omega_p$  is the LO frequency,  $\omega_0$  is the IF frequency, and  $m$  is any positive integer. Here, the frequency  $\omega_{+1}$  is the signal frequency and  $\omega_{-1}$  is the image frequency. When  $m$  is an even (odd) integer, the corresponding frequencies are called even (odd) "idle frequencies."